# The effect of two types of resorbable augmentation materials – a cement and an adhesive – on the screw pullout pullout resistance in human trabecular bone

Dan Wu [a,*], Michael Pujari-Palmer [a], Alicja Bojan [b], Anders Palmquist [c], Philip Procter [a], Caroline Öhman-Mägi [a], Stephen J. Ferguson [d], Per Isaksson [a], Cecilia Persson [a]

[a] *Department of Materials Science and Engineering, Uppsala University, Sweden*
[b] *Department of Orthopaedics, Sahlgrenska University Hospital Gothenburg, Sweden*
[c] *Department of Biomaterials, University of Gothenburg, Sweden*
[d] *Institute for Biomechanics, ETH Zürich, Switzerland*

ARTICLE INFO

ABSTRACT

Augmentation materials, such as ceramic and polymeric bone cements, have been frequently used to improve the physical engagement of screws inserted into bone. While ceramic, degradable cements may ultimately improve fixation stability, reports regarding their effect on early fixation stability have been inconsistent. On the other hand, a newly developed degradable ceramic adhesive that can bond with tissues surrounding the screw, may improve the pullout performance, ensure early stability, and subsequent bony integration. The aim of this study was to investigate failure mechanisms of screw/trabecular bone constructs by comparing non-augmented screws with screws augmented with a calcium phosphate cement or an adhesive, i.e. a phosphoserine-modified calcium phosphate. Pullout tests were performed on screws inserted into trabecular cylinders extracted from human femoral bone. Continuous and stepwise pullout loading was applied with and without real-time imaging in a synchrotron radiation micro-computed tomograph, respectively. Statistical analysis that took the bone morphology into account confirmed that augmentation with the adhesive supported significantly higher pullout loads compared to cement-augmented, or non-augmented screws. However, the adhesive also allowed for a higher injection volume compared to the cement. In-situ imaging showed cracks in the vicinity of the screw threads in all groups, and detachment of the augmentation materials from the trabecular bone in the augmented specimens. Additional cracks at the periphery of the augmentation and the bone-material interfaces were only observed in the adhesive-augmented specimen, indicating a contribution of surface bonding to the pullout resistance. An adhesive that has potential for bonding with tissues, displayed superior pullout resistance, compared to a brushite cement, and may be a promising material for cementation or augmentation of implants.

## 1. Introduction

In patients suffering from a bony fracture, either intramedullary implants or extramedullary plates used in combination with orthopedic screws are common solutions for surgical fixation. However, screw fixation in bone can be challenging, especially in poor quality bone, such as that found in patients with either osteopenic or osteoporotic bone. In the increasing elderly population, breakdown of screw constructs due to failure of surrounding bone may affect 3-25% of treated patients (Cornell, 2003; Katonis et al., 2011), resulting in reoperation and revision of the original implants. Therefore, techniques to improve the initial stability of screws are needed. Besides efforts related to new screw designs (Schliemann et al., 2019; Shea et al., 2014), augmentation with biomaterials such as polymethylmethacrylate (PMMA) and calcium phosphate cements (CPCs) have been applied to improve the physical engagement of the inserted screws (Bai et al., 2001; Elder et al., 2015; Larsson and Bauer, 2002; Larsson et al., 2012; Lattig, 2009; Leung et al., 2006; Liu et al., 2011; McKoy and An, 2000; Moore et al., 1997; Paré et al., 2011; Renner et al., 2004; Sarzier et al., 2002; Yu et al., 2011). Although augmentation with PMMA generally enhances the pullout
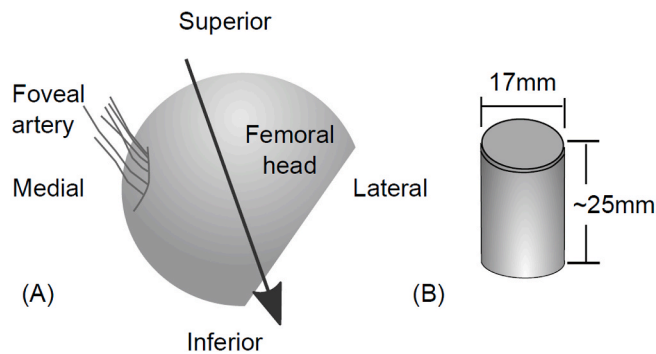
**Fig. 1.** Illustrations of (A) the sagittal view of the femoral with coring direction and (B) geometry of the resulting trabecular bone specimens.



**Fig. 2.** Dimensions of the aluminum screw used for the pullout tests.

strength, for instance, between 1.8 and 2.8-fold in vertebrae using pedicle screws (Liu et al., 2011; Renner et al., 2004; Sarzier et al., 2002), PMMA is not biodegradable and has limited potential for osseointegration (Elder et al., 2015). On the other hand, CPCs have the potential for remodeling and eventual replacement with bone (Larsson and Bauer, 2002; Seeherman et al., 2004), but are brittle materials, with limited mechanical strength, and variable improvements in pullout strength have been reported, ranging from significant improvement (although less than PMMA) (McKoy and An, 2000; Renner et al., 2004), to apparent reduction under certain conditions (Procter et al., 2015).

The pullout strength can possibly be improved by increasing the adhesion between the screw and trabecular bone, leading to a more even load distribution in the vicinity of the screw and along the threads. A transition from physical contact to adhesive bonding may further improve the shear and tensile fracture toughness at the interfaces and possibly reduce any screw migration. An improved material could be one that bonds the screw to the surrounding bone tissue for early stability, but that degrades over time, being replaced by the body's own tissue, creating an integrated bony network with similar mechanical properties as the bone tissue. Recently, a degradable, calcium phosphate based adhesive was developed, which can produce up to 40-fold higher bonding strength than commercial cyanoacrylates under wet-field conditions (Liu et al., 2019; Procter et al., 2019; Pujari-Palmer et al., 2018a). When combined with a phosphorylated amino acid, calcium phosphate cements gain novel properties, including adhesion. The adhesive used in the present study is a phosphoserine modified cement (Liu et al., 2019; Pujari-Palmer et al., 2018a). This adhesive could potentially improve early screw fixation. However, the various mechanisms underlying the adhesive effects, and how adhesion affects other physical properties such as augmentation strength, are not entirely understood, especially not on the micro scale.

The aim of this study was to investigate the reinforcement effects and failure mechanisms of a cement and an adhesive, both calcium phosphate-based, through screw pullout tests. Ex-situ screw pullout tests were first performed to quantify the ultimate pullout load, stiffness, and fracture energy of the three groups (non-augmented control, cement and adhesive). In addition, in-situ pullout tests were performed within a synchrotron radiation X-ray micro-computed tomograph (µCT), in order to visualize the reinforcement and failure mechanisms of the bone-screw connections.

## 2. Materials and methods

### 2.1. Bone specimens

Twenty femoral heads were obtained from redundant material from elderly patients undergoing hip arthroplasty due to femoral neck fracture. The anonymous collection of this material was performed according to the Ethical Review Board regulations in Gothenburg, Sweden,
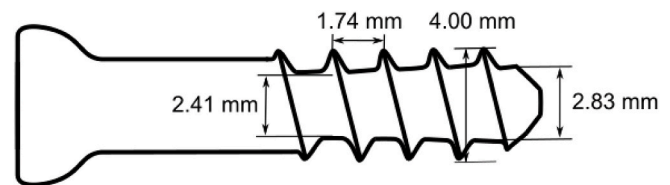
and the guideline for "good use of redundant tissue for research" was followed. Each bone sample was stored frozen at −80 °C and thawed overnight to room temperature before use. A cylindrical specimen (Ø17 mm) was cored from each femoral head, starting from the cartilage towards the femoral neck (Fig. 1). To ensure consistency in bone orientation, the specimen was taken above the foveal artery following the primary compression direction in femoral heads (Singh et al., 1970), except for the three specimens used in the pre-tests to establish a protocol which were taken randomly from two femoral heads. The inferior end of the bone cylinder was cut with a clinical oscillating saw, and a minimum length of 18 mm was ensured. The harvested trabecular cores were kept in phosphate buffered saline (PBS) solution to avoid dehydration. As bone volume fraction (BV/TV, i.e. bone volume over total volume) is the largest single determinant of bone strength (Gibson, 1985; Maquer et al., 2015; Seebeck et al., 2004; Tassani et al., 2010), the 21 specimens, which had a wide range of BV/TV (as determined by pre-scans of the material, see section 2.4), were assigned into three groups so that every group covered roughly the whole range.

### 2.2. Preparation of augmentation materials

The calcium phosphate cement (dicalcium phosphate dihydrate, brushite) was prepared by mixing the liquid and powder phases at a liquid-to-powder ratio of 0.25 mL/g, following a procedure described previously (Engstrand et al., 2014). In brief, the starting powder phase consisted of monocalcium phosphate monohydrate (MCPM, Scharlau, Spain) and beta-tricalcium phosphate (β-TCP, Sigma-Aldrich) at 45:55 mol%; the liquid phase was a solution of 0.5 M citric acid (Acros Organics).

The adhesive material, a phosphoserine modified calcium phosphate cement, hereafter referred to as adhesive for simplification, was prepared as described previously (Pujari-Palmer et al., 2018a). Briefly, alpha-tricalcium phosphate (α-TCP) and O-phospho-L-serine (Flamma) powders were mixed at a 30% molar ratio. The powders were combined with the liquid, a 20% (w/v%) solution of trisodium citrate (Fluka), at a liquid-to-powder ratio of 0.25 mL/g.

### 2.3. Screw insertion and augmentation

As the titanium alloy in orthopedic cancellous screws causes severe artifacts in both tube-based and synchrotron radiation µCT, screws made of a lighter material, namely aluminum, were used. The aluminum screws were custom-made in-house, resembling the geometry of titanium orthopedic cancellous screws (HB4), with an outer diameter of 4.0 mm and a total length of 22 mm. Due to limitations of the local workshop, the manufactured aluminum screws were half threaded, with a slightly conical inner diameter and smaller thread depths. Dimensions for the thread and inner diameter are shown in Fig. 2.

All bone specimens were manually predrilled to a diameter of 2.5 mm and a depth of 9 mm from the inferior ends. For the control group, screws were inserted directly into the bone. For the augmented specimens, the augmentation materials, i.e. the brushite cement and the adhesive, were prepared as described in the previous section. The cement or adhesive paste was transferred to a syringe (3 mL) with a spatula, and then injected immediately into the predrilled hole in the specimen. The injection was completed within about 90 s from the start of the cement
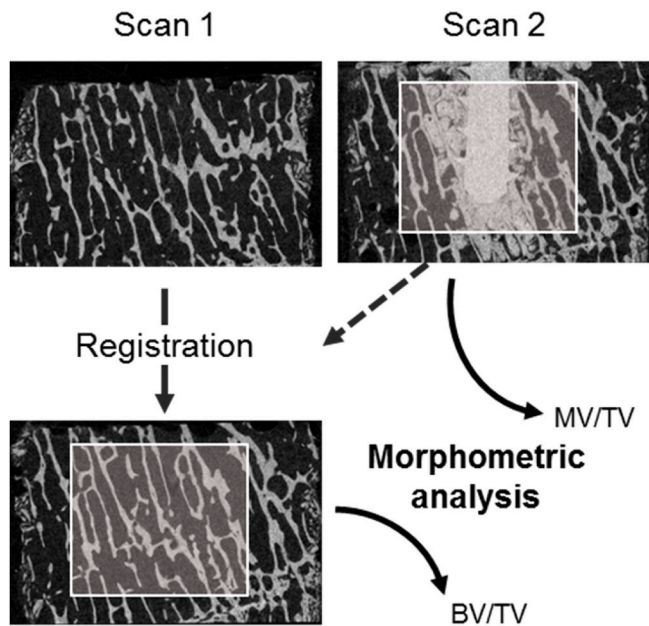
**Fig. 3.** The Scan 1 taken before screw insertion was registered to the Scan 2 taken after the screw insertion. Morphometric analysis was performed on the same volume of interest (VOI, denoted with the white square) on the two sets of scans to quantify different morphometric parameters. BV/TV stands for bone volume fraction, i.e. bone volume over total volume. MV/TV here denotes the volume fraction of trabecular bone plus augmentation material around the screw (see section 2.4).



**Fig. 4.** Illustration of the diameters of the volumes of interest (VOIs) around the screw and radial distance to the screw center.

preparation, and a screw was inserted immediately thereafter. The screw insertion took about 1 min, and the whole process was completed within 2 min and 30 s, well before the setting time of the material. A tighter time schedule was applied for the adhesive paste due to its shorter setting time. The injection of the adhesive was completed within 60 s from the start of the adhesive preparation, and the entire process finished at around 1 min and 20 s. All samples were allowed to set in air for 1 h, then immersed in PBS solution and kept at 37 °C until the next step.

For both materials, the target injection volume was 0.2 mL. However, the actual injection volume varied depending on the injectability of the augmentation material and the density/morphology of the bone specimen. Generally, a smaller volume of brushite cement could be injected, i.e. less than, or approximately, 0.1 mL.

### 2.4. Micro-computed tomography

Each specimen was scanned twice with a tube-based μCT scanner (Skyscan1172, Belgium): once before the screw insertion to determine the initial bone morphometric parameters (Scan 1, Fig. 3), and once after screw insertion to visualize the insertion and augmentation (Scan 2, Fig. 3). The same settings were used for the two scans, i.e. a tube voltage of 70 kV, a tube current of 141 μA, an aluminum and a copper filter, and an isotropic pixel size of 10 μm. The field of view was 20 mm in width and 13 mm in height, i.e. covering the part of the specimen containing the screw. The wet specimens were wrapped with preservation film to keep them moist during the scan.

Reconstructed images from Scan 1 were rigidly rotated to register to Scan 2 (Landmark Registration module, 3DSlicer), and then segmented with a global threshold for morphometric analyses (Fig. 3). The global threshold was selected based on a thickness calibration with aluminum-foil phantoms (Bruker, Belgium) and manually adjusted for the trabecular bone. The BV/TV was calculated within the volume of interest (VOI) by the '3D-Analysis' plug-in in CTan (Bruker, Belgium). Due to the inhomogeneity of the trabecular bone, BV/TVs in different VOIs were
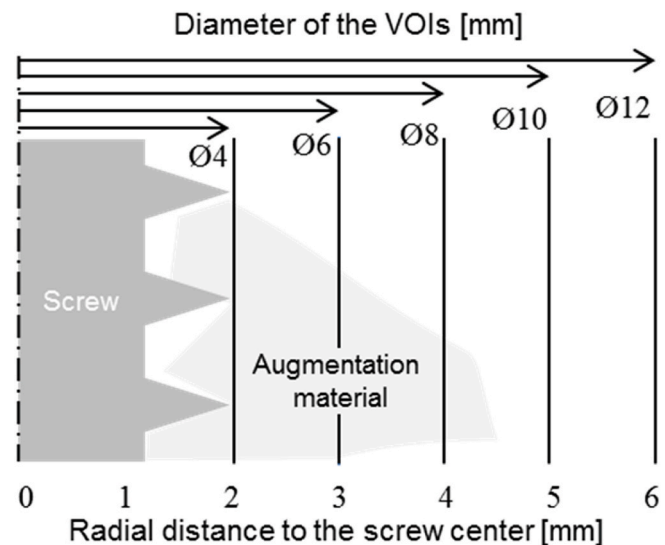
slightly different. To evaluate the effect of the VOI on the BV/TV and other parameters, five concentric cylindrical VOIs of increasing diameters were selected (Fig. 4), starting from 4 mm, i.e. the major diameter of the screw, to 12 mm, the largest diameter for the morphometric analyses, with an interval of 2 mm, and the same height of 10 mm.

The injection volume and the distribution of the augmentation materials in the radial direction were estimated based on the images from Scan 2 and the registered Scan 1, with the same threshold as before. The segmented volume in Scan 1 included trabecular bone, while the segmented volume in Scan 2 included bone, screw and augmentation material. The volume of screw was estimated from a μCT scan of the screw itself. Injection volume within a VOI was estimated by subtracting the volume of screw and trabecular bone from the segmented volume in Scan 2. Injection volumes in the ring regions between two consecutive VOIs were the increase in injection volume between the inner VOI and the outer VOI. Finally, the injection volume as a function of the radial distance to the screw center (Fig. 4) was estimated. The volume fraction of trabecular bone and augmentation material around the screw was denoted by MV/TV.

### 2.5. Ex-situ pullout testing

All specimens were subjected to pullout testing (Fig. 5) 24 h after insertion of the screws, using a universal testing machine (AGS-H, Shimadzu, Japan), equipped with a 5 kN load cell. A pre-load of 10 N was applied for a fixed specimen mounting, and the screws were pulled out of the trabecular bone at a constant cross-head rate of 1 mm/min, to allow for accurate detection of the failure point in the brittle material. The peak load obtained is hereafter defined as the pullout load. The specimen stiffness was determined as the slope of the straight line that best fit the force-displacement curve in its linear part before onset of nonlinearity, and then compensated for system compliance, which was tested by blocking the movement of the clamp with a metal plate (Fig. 5) and pulling upwards at the same cross-head rate until 1 kN. The fracture energy was calculated as the area under the load-displacement curve until the pullout load was reached. To test the procedure, pre-tests were performed on three specimens taken from two femoral heads.

### 2.6. In-situ pullout testing

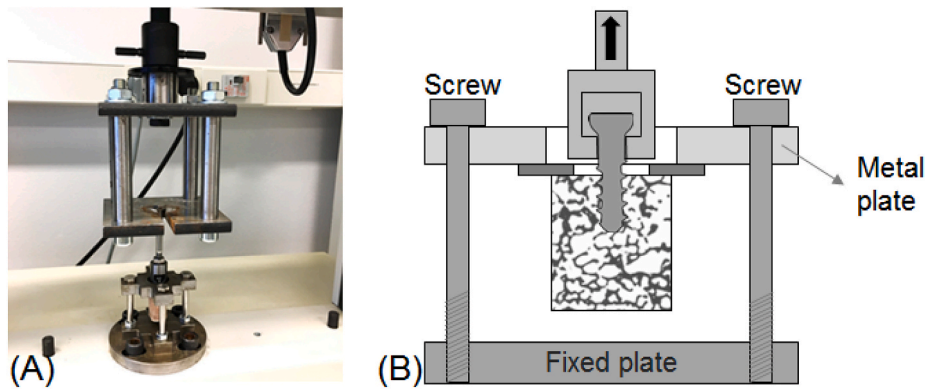To visualize the fracture behavior of the trabeculae as well as that of

**Fig. 5.** Illustration of the setup for ex-situ pullout testing.

the augmentation materials and their combination, in-situ testing combining a stepwise screw pullout with synchrotron radiation X-ray based μCT was performed at the TOMCAT beamline at the Swiss Light Source (SLS) (Paul Scherrer Institute (PSI), Switzerland). Five specimens were tested, two augmented with brushite cement, one with adhesive and two non-augmented control specimens. The five specimens for the in-situ testing were named in the form of 'Augmentation material-in-Specimen number', for instance Cement-in-1 and Control-in-1, where 'in' denotes in-situ, and 'Cement'/'Control' for the cement augmentation or no augmentation.

Some specimen preparation procedures were adjusted to adapt to the facilities at the beamline and are therefore listed in this section. The trabecular bone cores were taken from human femoral bone (ethics committee approval EK-29/2007, Zürich) and were of smaller size, specifically a diameter of Ø15 mm and a height of 15 mm. To ensure injectability of the augmentation materials, the bone specimens underwent ultrasonic bath cleaning for around 30 min. Here, the bone specimens were immersed in a solution of PBS, 70% ethanol and a small amount of detergent for cleaning. The liquid-to-powder ratio of the brushite cement was reduced slightly to 0.225 mL/g to decrease the risk of excessive cement penetration and little cement around the screw. The insertion depth of the screw was limited to 6 mm due to the smaller size of the specimens and the limit of the loading rig. The augmented bone specimens were immersed in PBS solution after 15–20 min setting in air, and kept in room temperature for about 12–24 h before testing. The adhesive samples were prepared in the same manner as the cements.

In the synchrotron radiation μCT, the voxel size was set at 5.2 μm as a compromise between resolution and a sufficiently large field of view (FOV, $12.5 \times 3.9 \, mm^2$) around the inserted screw. Two-stack scans were performed to capture the total depth of insertion. A 27 keV beam energy was selected with an exposure time of 220 ms, and 801 projections were taken with an angular step of 0.23°. The resulting scanning time per loading step was approximately 10 min. After scanning, the acquired projection images were reconstructed into cross sectional images with

an ImageJ extension. The largest diameter of the VOI was 10 mm due to the smaller FOV in the synchrotron radiation μCT.

The pullout testing was performed with a material testing stage (MTS1, Bruker, Kontich, Belgium) adapted for use in the synchrotron radiation μCT. The uniaxial load was measured by a 1 kN load cell (Futek, Southern California, United States), and the displacement was read from the materials testing stage. A small pre-load was applied to guarantee a fixed specimen mounting. Loading rate varied between 0.01 and 0.36 mm/min, as limited by the testing stage. Screws were pulled out stepwisely allowing μCT scans to be performed during the holding time. For each step the displacement varied between 0.05 and 0.15 mm, and the scan started around 10 s after the loading. The pullout load was defined similarly to the ex-situ testing, while stiffness and fracture energy were not calculated for this stepwise test.

### 2.7. Statistical analysis

IBM SPSS Statistics (v.22 IBM Corp, Armonk, NY, USA) was used with the results from the ex-situ testing to analyze the variance. Linear regression was performed on the control group to determine the parameters for the statistical analysis afterwards. To select the BV/TV from various VOIs, linear regression between the pullout load and the BV/TVs was performed. Coefficient of determination $R^2$ and root mean square error (RMSE) were used to compare the explanatory power of the regression models.

As the one-way ANOVA analysis showed no significant difference in the pullout properties between the pre-test specimens, normalized with BV/TV, and the control group, the three specimens from the pre-test were therefore included in the control group hereafter. Pullout properties, i.e. pullout load, stiffness and fracture energy, were normalized by the BV/TV, and one-way ANOVA analyses with Tukey HSD as post hoc were performed to compare these properties between the three groups (control, cement and adhesive). As a difference in the injection volume was found between the augmentations with cement and adhesive, the
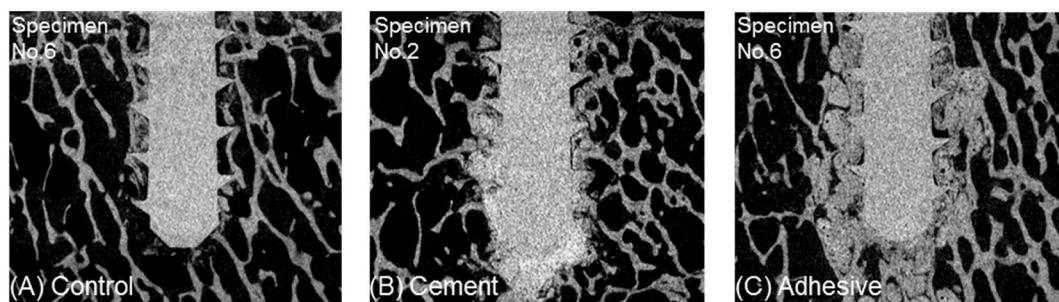


**Fig. 6.** Section views from Scan 2 showing the inserted screw and the distribution of the augmentation materials in ex-situ specimens in three groups: (A) control, (B) cement, and (C) adhesive.
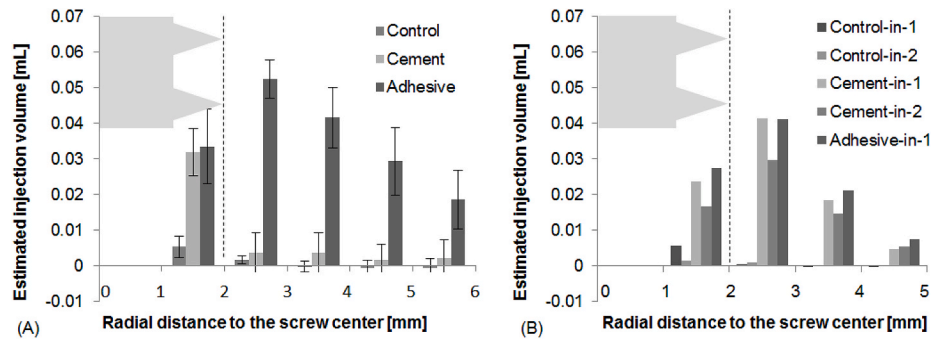
**Fig. 7.** Estimated injection volume as a function of distance to the screw center for (A) the ex-situ specimens and (B) the in-situ specimens. The edge of the outer threads at a radial distance of 2 mm is denoted with a dash line. The non-zero value for control specimens are due to bone debris.
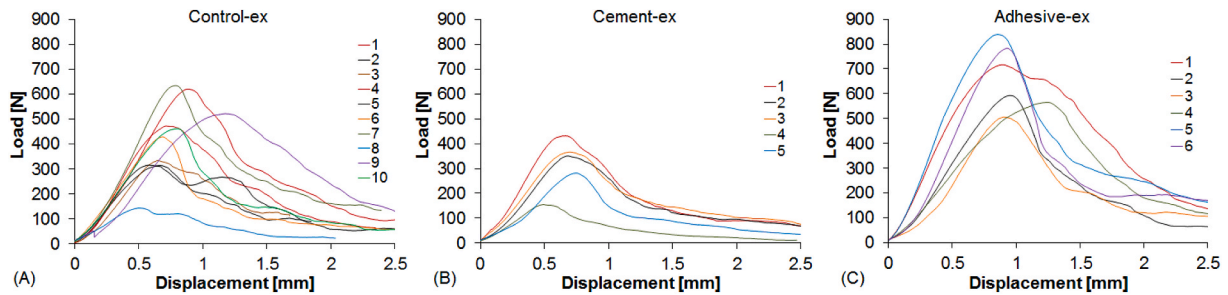


**Fig. 8.** Load-displacement curves from the ex-situ pullout testing for the three groups: (A) control, (B) cement, and (C) adhesive.

**Table 1**
Volume fractions and pullout resistance of all specimens in the ex-situ pullout testing.

| Group | Specimen number | BV/TV[a] | MV/TV[b] | Pullout load | Stiffness | Fracture energy |
|---|---|---|---|---|---|---|
| | | % | % | N | N/mm | N·mm |
| Control | 1[c] | 26.6 | 26.2 | 472.3 | 1845.9 | 171.9 |
| | 2[c] | 25.3 | 25.3 | 314.0 | 968.5 | 116.1 |
| | 3[c] | 24.1 | 25.7 | 333.8 | 1045.9 | 102.7 |
| | 4 | 32.2 | 29.2 | 620.0 | 1738.7 | 262.0 |
| | 5 | 24.1 | 21.9 | 315.5 | 1137.2 | 99.7 |
| | 6 | 24.9 | 23.2 | 428.8 | 1147.4 | 155.1 |
| | 7 | 39.9 | 34.5 | 634.5 | 2386.1 | 244.5 |
| | 8 | 18.1 | 20.3 | 143.5 | 394.0 | 40.2 |
| | 9 | 33.2 | 31.0 | 521.8 | 1035.4 | 321.6 |
| | 10 | 27.2 | 27.4 | 461.8 | 1234.7 | 196.8 |
| Cement | 1 | 23.6 | 26.9 | 431.5 | 1666.2 | 146.4 |
| | 2 | 22.7 | 30.8 | 351.0 | 1020.2 | 118.4 |
| | 3 | 28.5 | 27.3 | 366.5 | 1051.9 | 136.4 |
| | 4 | 18.9 | 25.0 | 155.5 | 456.0 | 39.4 |
| | 5 | 25.7 | 35.2 | 281.5 | 734.4 | 101.0 |
| Adhesive | 1 | 31.2 | 49.5 | 716.8 | 2680.7 | 368.4 |
| | 2 | 31.9 | 43.6 | 593.0 | 1412.2 | 281.2 |
| | 3 | 24.7 | 42.2 | 506.0 | 1447.5 | 205.9 |
| | 4 | 23.1 | 34.7 | 565.3 | 915.4 | 406.1 |
| | 5 | 29.8 | 47.0 | 838.3 | 4399.6 | 388.5 |
| | 6 | 27.0 | 38.2 | 783.3 | 3012.6 | 353.4 |
| Control | Mean | 27.6 ± 6.1 | 26.5 ± 4.3 | 424.6 ± 151.6 | 1293.4 ± 556.7 | 171.0 ± 86.4 |
| Cement | Mean | 23.9 ± 3.6 | 29.0 ± 4.0 | 317.2 ± 105.0 | 985.7 ± 450.7 | 108.3 ± 42.3 |
| Adhesive | Mean | 27.9 ± 3.6 | 42.5 ± 5.5 | 667.1 ± 132.0 | 2311.3 ± 1303.2 | 333.9 ± 76.1 |

[a] Bone volume over total volume, calculated from Scan 1 (before screw insertion) with VOI of diameter 4 mm.

[b] Material volume over total volume, calculated from Scan 2 (after screw insertion) with VOI of diameter 12 mm.

[c] The three specimens for the pre-tests were taken randomly from two femoral heads, specifically, specimens number 2 and 3 were from one femoral head, tested about 5 h after insertion, and kept at room temperature.

pullout properties were also normalized by MV/TV, and one-way ANOVA was performed. A statistically significant difference was confirmed when the probability value $p$ was less than 0.05.

## 3. Results

### 3.1. Material augmentation

The distribution of the augmentation materials in the ex-situ bone specimens is exemplified in Fig. 6, and the estimated injection volume as a function of distance from the screw center, was calculated for all specimens (Fig. 7). Bone debris was noticed between the threads and included in the estimation of injection volume in Fig. 7. The variations in injection volume far away from the screw center reflect registration error by the 'Landmark Registration' method. As expected, both augmentation materials concentrated near the screw, but penetrated to different extents radially. In the ex-situ specimens, the volume of cement in the space outside the screw major diameter (radial distance > 2 mm) was quite limited. However, adhesive was found at a radial distance larger than 5 mm, with similar injection volume between the threads but much higher volume outside the screw major diameter. In the in-situ specimens, the penetration depth of the cement was similar to the adhesive, and both were found at a distance of up to 5 mm. The injection volumes were slightly lower in specimens augmented with cement than the one with adhesive.

**Table 2**
Coefficient of determination ($R^2$) and root mean square error (RMSE) in the linear regression analyses between the pullout load and BV/TV from various VOI with specimens in the control group, not including the ones in the pre-test.

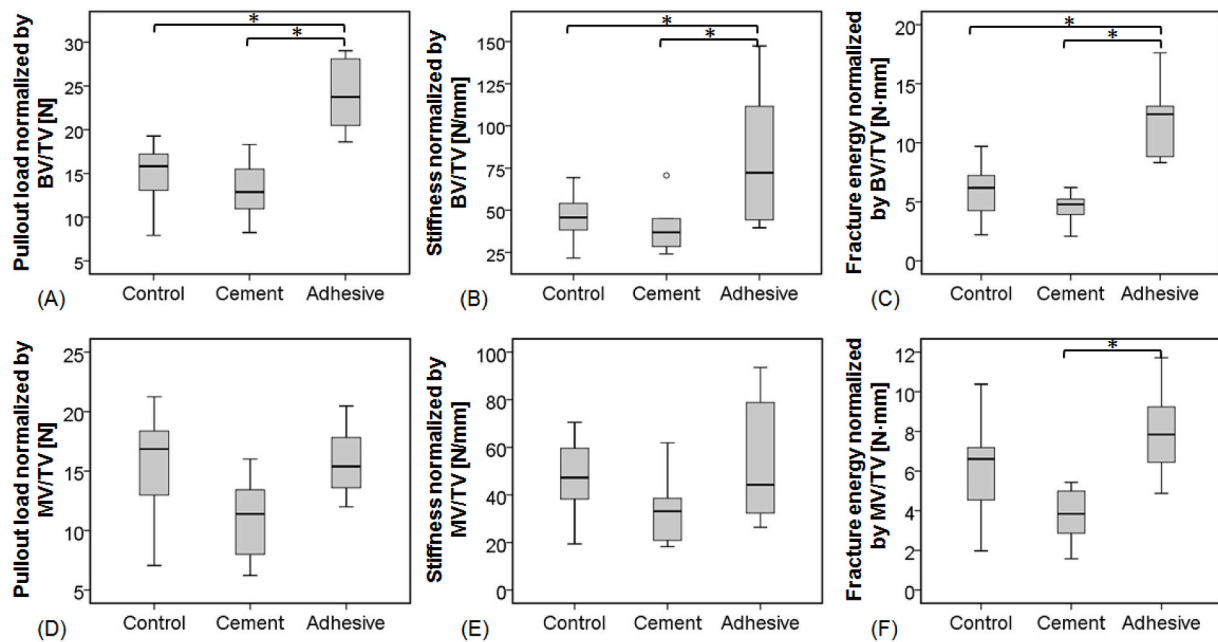| BV/TV | $R^2$ | RMSE (N) |
|---|---|---|
| VOI Ø4 | **0.858** | **71.6** |
| VOI Ø6 | 0.856 | 72.1 |
| VOI Ø8 | 0.849 | 73.8 |
| VOI Ø10 | 0.836 | 76.9 |
| VOI Ø12 | 0.814 | 82.0 |

**Fig. 9.** Pullout load, stiffness and fracture energy of the ex-situ specimens, normalized by BV/TV (VOI Ø4) and MV/TV (VOI Ø4). The asterisk mark (*) denotes a statistically significant difference between two compared groups (values for each specimen are presented in Supplementary Table S2).
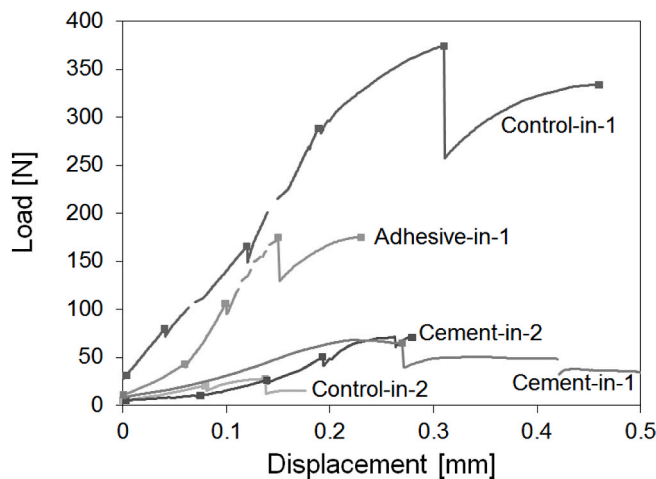


**Fig. 10.** Load and displacement from the in-situ pullout testing assuming a constant loading rate for each specimen. Square dots denote where the μCT scans were taken.

### 3.2. Pullout strength

Load-displacement curves from the ex-situ pullout tests are shown in Fig. 8 and the pullout load and stiffness are summarized in Table 1, together with BV/TV from Scan 1 and MV/TV from Scan 2.

As the BV/TV calculated in the VOI of diameter of 4 mm showed the highest correlation to the pullout load (Table 2), it was used for the following statistical analyses. When normalized by the BV/TV, the pullout load in the adhesive group was significantly higher than the control group ($p < 0.001$) and the cement group ($p < 0.001$), though no significant difference was found between the cement and control groups ($p = 0.640$) (Fig. 9A). The stiffness in the adhesive group was significantly higher than the cement ($p = 0.048$) and the control group ($p = 0.039$), but no difference was found between the cement and the control group ($p = 0.994$) (Fig. 9B). A similar trend was found for the fracture energy, with the adhesive being significantly higher than the cement ($p < 0.001$) and control group ($p < 0.001$), and no significant difference

**Table 3**
Volume fractions and pullout load of all specimens in the in-situ pullout testing.

| | BV/TV[a] | MV/TV[b] | Pullout load |
|---|---|---|---|
| | % | % | N |
| Control-in-1 | 31.7 | 33.9 | 374.2 |
| Control-in-2 | 17.6 | 18.2 | 27.6 |
| Cement-in-1 | 20.4 | 39.6 | 68.1 |
| Cement-in-2 | 25.8 | 39.8 | 71.2 |
| Adhesive-in-1 | 21.3 | 41.8 | 175.0 |

[a] Bone volume over total volume, calculated from Scan 1 (before screw insertion) with VOI of diameter 4 mm.
[b] Material volume over total volume, calculated from Scan 2 (after screw insertion) with VOI of diameter 10 mm.

between the cement and the control group ($p = 0.538$) (Fig. 9C). When normalized by the MV/TV, a significant difference was only found for the fracture energy, between the adhesive and cement groups ($p = 0.010$) (Fig. 9D-F).

### 3.3. Failure mechanism

Stepwise pullout testing was performed inside a synchrotron radiation μCT to capture the failure during loading. The load and displacements in the in-situ pullout are summarized in Fig. 10 and Table 3. A small amount of relaxation in the load was noticed during the holding state as well as larger drops of loads in the second to last steps of Control-in-1 and Adhesive-in-1. Due to the limited sample size in the in-situ testing and more similar spreading of the material, pullout loads from the in-situ testing were not compared with the ex-situ testing. While more samples would be needed for verification, it cannot be excluded that the less prominent advantage of the adhesive compared to the cement in the in-situ testing is partly due to the more similar spreading of the materials for that testing (Fig. 7). However, the in-situ testing had other limitations that may have contributed to generally lower loads (see section 4.3).

Slices of the peri-implant region from several loading steps are presented for each specimen (Figs. 11-15). For specimens without augmentation, it is clear that some screw threads wedged into the
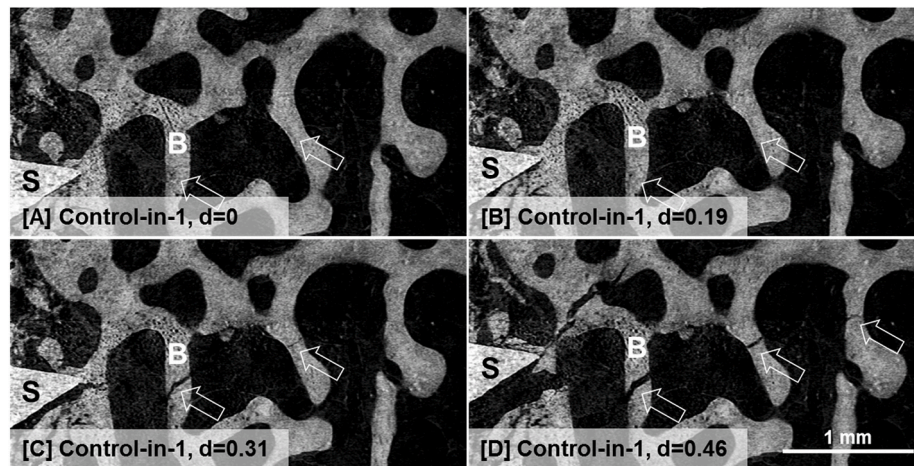
**Fig. 11.** Cracks across several trabeculae during screw pullout from Control-in-1 at four loading steps of displacement (A) 0 mm, (B) 0.19 mm (C) 0.31 mm and (D 0.46 mm 'B' denotes bone, 'S' denotes the screw, and 'd' in the subtitles denotes applied displacement in mm.
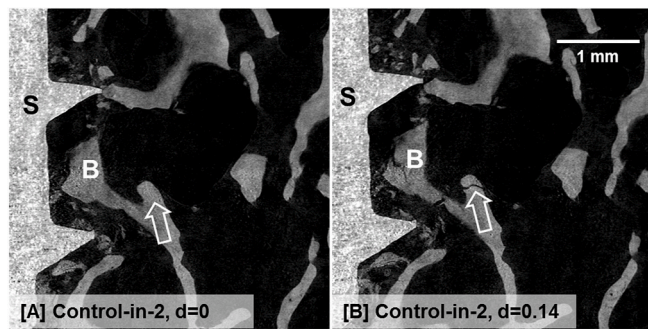


**Fig. 12.** Cracks during screw pullout from Control-in-2 at (A) pre-load and (B) peak load. 'B' denotes bone, 'S' denotes screw, and 'd' in the subtitles denotes applied displacement in mm.

trabecular bone, creating notches in the trabecular bone and induced cracks. In Control-in-1, as exemplified in Fig. 11, a crack initiated at the thread crest, and propagated across several trabeculae. When more displacement was applied, the crack advanced. In Control-in-2, local

failure right around the thread crests but no cracks across several trabeculae were observed (Fig. 12). When cement was injected, both cement and trabeculae failed during the screw pullout, and bone debris was packed between the threads (Fig. 13); cracks across several trabeculae were not observed in Cement-in-1 and Cement-in-2. When the trabecular specimen were augmented with adhesive, cracks not only propagated across bone and adhesive from the thread crests outwards (Fig. 14), but also initiated at the peripheries of bone-adhesive composite (Fig. 15).

Fig. 16 shows the screw detaching with the surrounding bone, cement or adhesive at the screw tip during the pullout. Complete detachment occurred between the screw and bone in Control-in-1, and between the bone and cement in Cement-in-1. However, for at least one interface between the screw and the adhesive, cracks grew partially across the adhesive following the profile of the screw tip, with some adhesive sticking to the thread surface (Fig. 16F).

When cracks reached the interface between the bone and the augmentation material, interfacial detachment of the cement with the trabecular bone (Fig. 17A-D) was observed, as well as debonding between the adhesive and the bone (Fig. 17E-F), as consequences of the interfacial initiated delamination cracks. It was also observed that a
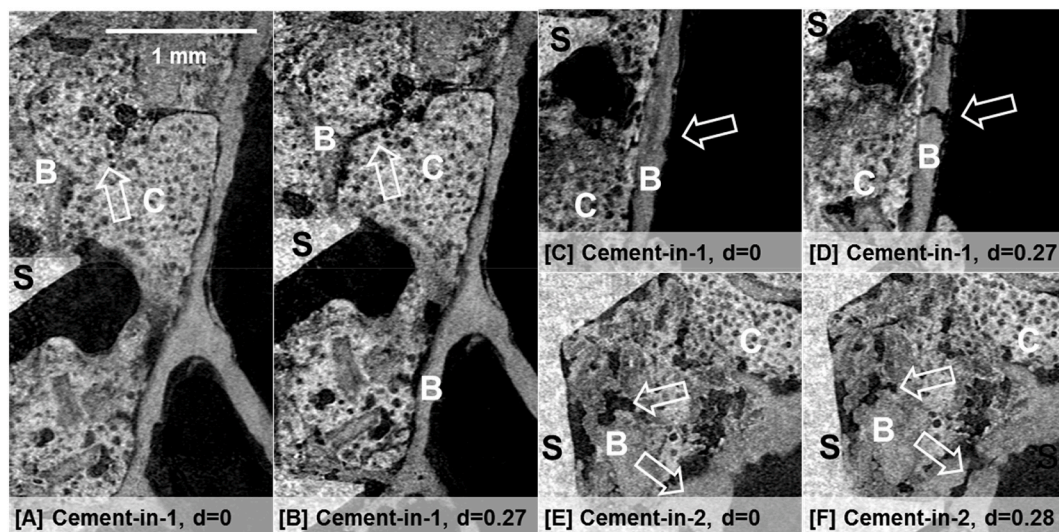


**Fig. 13.** Cracks in bone and cement during screw pullout from Cement-in-1 and Cement-in-2, showing (A-B) cracks initiated at the bone-cement interface, (C-D) failure of trabecular bone, and (E-F) bone debris packed between the threads. 'B' denotes bone, 'C' denotes cement, 'S' denotes screw, and 'd' in the subtitles denotes applied displacement in mm.
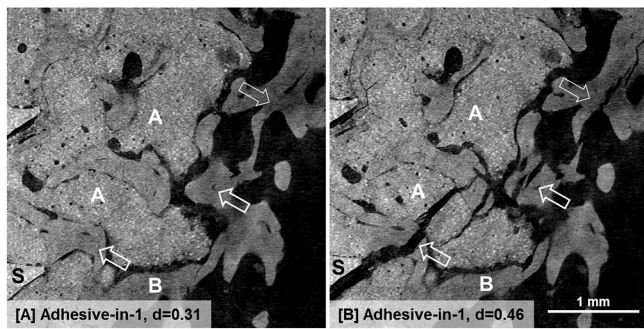
**Fig. 14.** Cracks across trabeculae and adhesive during screw pullout from Adhesive-in-1 at two loading steps of displacement (A) 0.31 mm and (B) 0.46 mm 'A' denotes adhesive, 'B' denotes bone, 'S' denotes screw, and 'd' in the subtitles denotes applied displacement in mm.

second crack initiated and grew from the bone-adhesive interface into the trabecular bone even though the main crack followed the interface (Fig. 17G-H).

## 4. Discussion

This study compared screw fixation, with and without augmentation with a brushite cement or an adhesive cement material, by axial pullout tests from human trabecular bone. Since bone volume fraction (BV/TV) explained much of the variation in the pullout load without augmentation, it was used to account for the structural differences in bone specimens. The ex-situ pullout resistance showed a significant improvement after augmentation with the adhesive in trabecular bone, but no improvement with the brushite cement, compared to the control, non-augmented group. It should be noted, however, that in general more adhesive could be injected than cement, and tended to spread further away from the screw. In-situ imaging revealed a difference in the trabecular behavior for augmentation with the two ceramics (cement and adhesive). Cracks propagated from the thread crests outwards radially and from the peripheries of the bone-adhesive composite towards the screw after augmentation with the adhesive. Bonding between the adhesive and the screw was observed, as well as crack growth from

the bone-adhesive interface into the trabecular bone, suggesting engagement of trabecular bone in load sharing during pull-out testing. The discussion below starts with factors affecting the screw pullout properties which are categorized into bone volume fraction and augmentation materials. Their effect on the crack initiation and propagation is then discussed, based on the in-situ images.

### 4.1. Effect of bone volume fraction and augmentation materials on pullout strength

The high correlation between pullout load and BV/TVs confirmed the earlier reported main effect of BV/TV (Piper and Brown, 2016; Wirth et al., 2011) or bone mineral density (Okuyama et al., 2001; Reitman et al., 2004) on the pullout strength of screw fixation. The slightly higher correlation with the local BV/TV in the VOI closest to the screw showed a contribution of bone in the direct vicinity of the screw to the pullout resistance. This is probably due to the highly localized strains in the trabeculae in contacts with the screws. Generally, a higher BV/TV near the screw means higher likelihood of physical contact between trabeculae and the screw thread, leading to a higher resistance to pullout. The bone density farther away from the screw center is less likely to contribute heavily to the pullout strength, making the difference in sample dimensions less important. Furthermore, it has been reported that the cortical thickness, when above 1.5 mm, has a significant effect upon fixation (Seeherman et al., 2004). The effect of the cortical layer is more complex to assess when used with augmentation materials, depending upon the location of the augmentation and the contact between the augmentation materials and the cortical bone (Wang et al., 2009). The cortical layer was therefore not included in this study to limit the number of variables.

When the pullout properties were normalized by BV/TV, augmentation with the brushite cement showed no significant difference in pullout load, i.e. a slightly worse result than those generally reported previously, as an increase has been reported in various studies, for instance, 1.7-fold in a femoral neck fracture fixation (Stankewich et al., 1996), 1.6-2 fold with pedicle screws in human vertebrae (Pishnamaz et al., 2018; Renner et al., 2004), in rabbit femurs (Larsson et al., 2012), and restored to baseline in a revision after screw failure (Moore et al., 1997). However, a decrease in pullout strength by cement augmentation
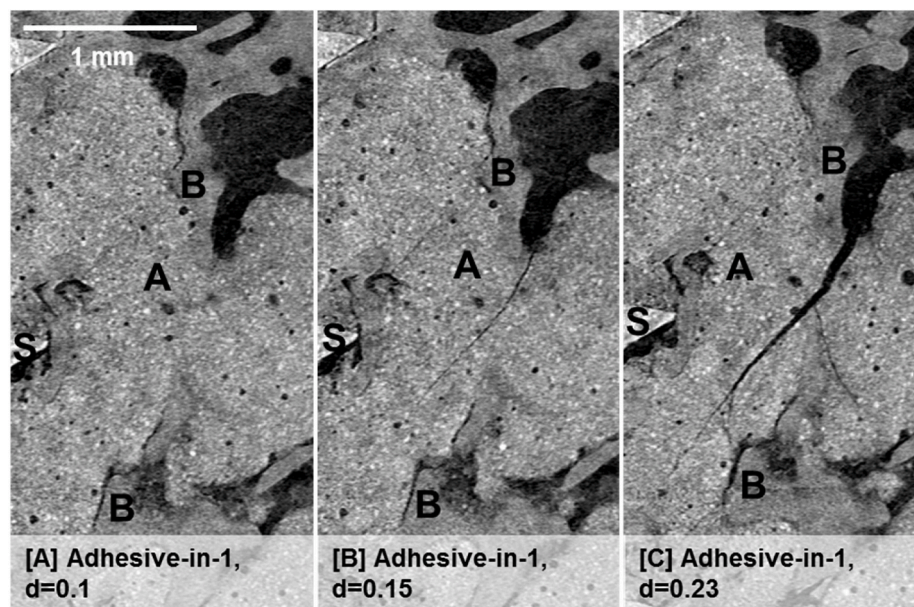


**Fig. 15.** Induced cracks in bone and adhesive during screw pullout from Adhesive-in-1, showing a crack that initiated at the periphery of the bone-adhesive composite and then propagated towards the screw. 'A' denotes adhesive, 'B' denotes bone, 'S' denotes screw, and 'd' in the subtitles denotes applied displacement in mm.
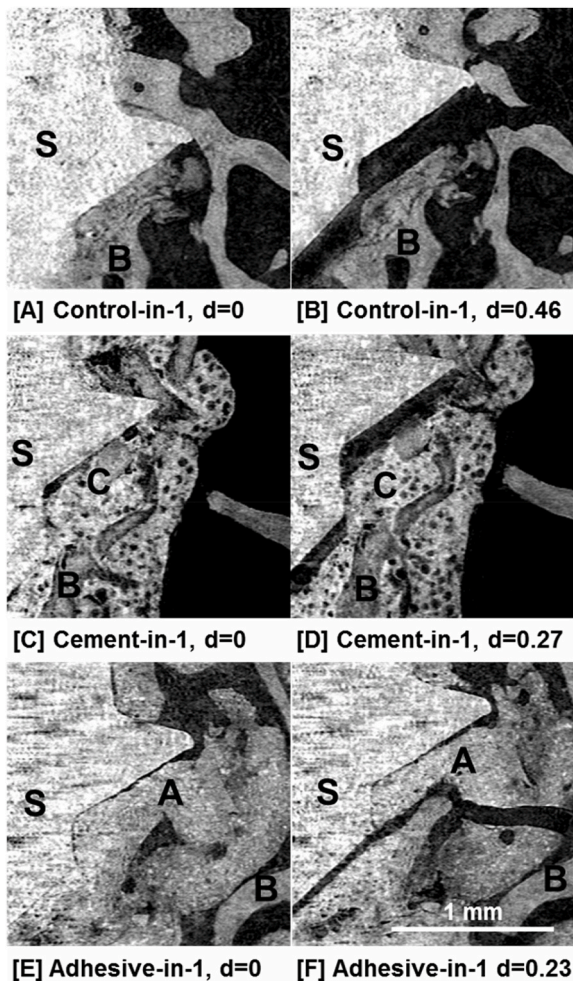
**Fig. 16.** Detaching of screw with (A-B) bone and (C-D) cement; (E-F) adhesive sticking to the thread proximal surface near the screw tip. 'A' denotes adhesive, 'B' denotes bone, 'C' denotes cement, 'S' denotes screw, and 'd' in the subtitles denotes applied displacement in mm.

has also been observed in some paired human cadaver femurs, although a generally increased pullout strength after augmentation was reported in this study (Procter et al., 2015). In contrast, augmentation with the adhesive showed significant improvement in the pullout load compared to the control, specifically, 1.6-fold higher. This is comparable to the enhancement after augmentation with cement as reported in the aforementioned literature, and somewhat worse than augmentation with PMMA in vertebrae (1.8-2.8 fold (Liu et al., 2011; Renner et al., 2004; Sarzier et al., 2002)).

One of the reasons for a difference in reinforcement achieved with different materials could of course be the mechanical properties of the augmentation bulk materials. Compared to the cement, the adhesive had higher compressive strength and lower bulk shear strength (see supporting information). The compressive strength of brushite cement has been reported to show a positive correlation to the pullout load in synthetic models if sufficient cortical thickness is present, but poor correlation if not (Pujari-Palmer et al., 2018b). With the cortical layer excluded in our model, the contribution of higher compressive strength in the adhesive might be limited. However, synthetic models are quite different from real bone in both structure and mechanical properties. Additionally, how the difference in bulk shear strength between the two ceramics would affect the pullout load is unclear.

Other factors related to the augmentation, which might affect the pullout resistance, are the injection volume, and the level of

augmentation in the radial direction and between the threads. The injection volume of cement in the ex-situ testing was smaller than the adhesive, which likely affected the ex-situ pullout resistance. The general linear model analysis with ex-situ specimens showed that the injection volume was not a significant factor to the pullout load (Supplementary Table S3). This is however likely due to the large difference in injection volumes between the two augmentation materials for the ex-situ tests, i.e., the effect of injection volume could be included implicitly in the 'group' variable. Although the injection volume has not been detected as a significant factor to the pullout resistance (Frankel et al., 2007; Paré et al., 2011), there might be a critical threshold value for the cement to improve the pullout performance as reported in PMMA-augmented pedicle screws (Paré et al., 2011). Indeed, when the pullout properties were normalized with MV/TV, which was a reflection of both BV/TV and injection volume in the specimen, significant differences were not found in most cases, though the cement group showed generally lower properties. However, the results should be interpreted with caution, as a linear relation between pullout resistance and MV/TV was assumed. Connected to the injection volume, there was much less cement than adhesive at a distance from the threads (>2 mm, Fig. 7). The increased radial augmentation might be another reason for the enhancement in pullout load for the adhesive group (Brown et al., 2013). Moreover, the augmentation materials did not fill all the space around the screw, leaving voids between the threads (Fig. 13). This phenomenon was more obvious in Cement-in-1 and Cement-in-2, which had higher porosities than the Adhesive-in-1, after augmentation in the region closely around the screws. These voids would weaken the apparent strength of the composite between the threads and reduce the contact surface to the threads, resulting in less pullout resistance compared to a more complete augmentation. The better, overall distribution of augmentation material suggests that there is an advantage in injectability with the adhesive, compared to the brushite cement used.

### 4.2. Effect of augmentation materials on the fracture behavior

The crack propagation across several trabeculae in the Control-in-1 (Fig. 11) is similar to the typical cracks observed in brittle foams (Gibson and Ashby, 1997). In Control-in-2, which had approximately half the BV/TV as Control-in-1, cracks were more concentrated around the threads. Long cracks across several trabeculae were not observed here, neither in the two samples augmented with the cement, although, they did appear in Adhesive-in-1. The adhesive filled the space between trabeculae, bonding and bridging the trabeculae, causing the crack to propagate through the bone and the adhesive, though this was sometimes disturbed by the bone-adhesive interface (Fig. 14).

In Adhesive-in-1, cracks at both the vicinity of threads and the peripheries of the injected adhesive were observed, indicating a more even load distribution in the peri-implant region. Digital volume correlation and finite element analyses showed that without augmentation, the stress concentrated near the threads when axial pullout load was applied (Joffre et al., 2017; Wirth et al., 2011). When a perfectly-solid ceramic bulk was injected to the screw tip as modelled by finite elements, the stress mainly concentrated at the peripheries of the bulk material (Wang et al., 2009). Though in practical tests, this perfect/simplified situation was never reached, the adhesive injected around the screw performed more similarly towards a solid ceramic than the cement did. Despite the possible effect of the different material properties and the augmentation between the adhesive and the cement as discussed in section 4.1, one contribution to the improved performance with the adhesive might be the bonding strength of the adhesive.

The bonding effect was reflected by the in-situ images (Fig. 16). At the proximal surface of the thread near the screw tip, the screw detached from the surrounding trabecular bone in Control-in-1 and Cement-in-1. However, in Adhesive-in-1, though the screw tip detached from the adhesive, a piece of adhesive stuck to the proximal surface of the thread, demonstrating to some extent the adhesion between screw and the
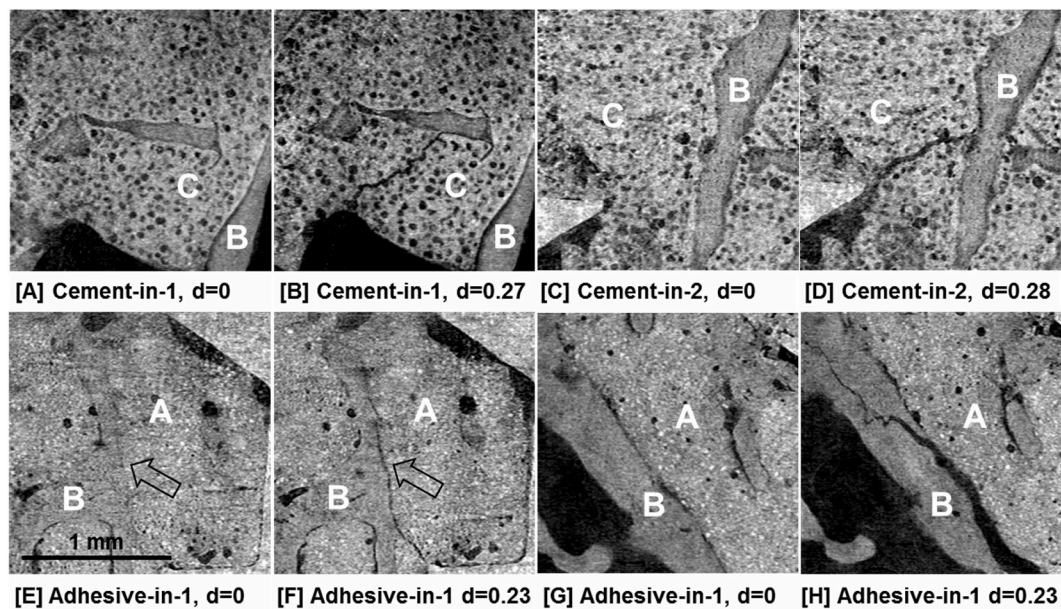
**Fig. 17.** Cracks followed the interface in (A-B) Cement-in-1, (C-D) Cement-in-2, and (E-F) Adhesive-in-1. A deviation of crack from the bone-adhesive interface was presented in (G-H) Adhesive-in-1. Cracks were noticed in the cement. 'A' denotes adhesive, 'B' denotes bone, 'C' denotes cement, and 'd' in the subtitles denotes applied displacement in mm.

adhesive, as reported between the bone-bone and steel-steel interface by co-authors of the current study (Pujari-Palmer et al., 2018a).

The adhesion affected cracks near the interface between bone and the augmentation material, as shown in Fig. 17. Interfacial delamination was observed in the bone-cement, as well as bone-adhesive interface, likely due to the generally low adhesion of the interfaces. However, cracks that initiated at the interface and grew into the trabecular bone were only observed in the adhesive augmented samples, at the bone-adhesive interface, reflecting a stronger bonding strength and load sharing than the bone-cement interface. This phenomenon occurred in accordance with the reported effect of adhesion on the fracture of several bone composites (Lucksanasombool et al., 2003), where subsequent fracture throughout the bone was observed for composites that form chemical (covalent or ionic) bonds, while bone-PMMA composites that lack chemical bonding had the greatest amount of distinct interfacial failure.

### 4.3. Limitations

One of the limitations of this study is that the range of bone densities was limited; low density samples, such as those for osteopenic and osteoporotic bone, were not available. Performance of the augmentation materials outside the present study's bone density range cannot be inferred based upon the linear correlation with bone morphology. Strategies intended to enhance screw fixation may perform differently between normal and osteoporotic bones. However, augmentation with calcium phosphate cement significantly improved the stability of intertrochanteric fractures fixed with a proximal femoral nail and reduced overall failure rates (Kim et al., 2018). Such fractures are usually associated with osteoporotic bone. Additionally, augmentation with PMMA was reported to increase stability in osteoporotic vertebrae but not in non-osteoporotic specimens (Hoppe et al., 2014).

Besides the low sample number in the in-situ tests, due to the limited beamtime available at the synchrotron light source, the specimen preparation and testing were not exactly the same for the in-situ testing as the ex-situ testing. Specimens in the in-situ testing were subjected to a higher dose of X-rays, which has been reported to affect the fracture behavior of bone (Barth et al., 2011; Peña Fernández et al., 2018). The insertion depth was limited to 6 mm, possibly leading to additional

variation in the pullout load. The specimens augmented with the cement showed more radial augmentation than the ex-situ test due to the cleaning process. Furthermore, the loading rate was not comparable to the ex-situ testing due to differences in the testing hardware. Therefore, the difference in crack propagation during the in-situ test might not fully explain the pullout strength in the ex-situ testing.

In addition, due to the limitation of the manufacturing method (local workshop), the surface roughness of the aluminum screws was not identical (rougher) to the titanium orthopedic screws. The friction between the aluminum screws and the trabecular bone/augmentation materials was therefore expected to be slightly higher than that of the titanium screws. Moreover, the pullout testing was performed ex-vivo at 12 h or 24 h after the screw insertion. Only the effect of augmentation materials on the primary stability was studied. In the clinical application, the two augmentation materials might have different long-term effects on the stability.

## 5. Conclusions

This study showed no significant difference between augmentation with the brushite cement and no augmentation when the augmentation volume is low. Better augmentation in terms of volume and distribution was found with the ceramic adhesive than the brushite cement, and the axial pullout load was significantly increased as compared to the cement case herein, as well as compared to no augmentation. In-situ imaging during the screw pullout captured the fracture behavior inside the specimens. Besides the cracks in the vicinity of the threads as in the trabecular bone augmented with the cement or no augmentation, cracks were also observed at the peripheries of the bone-adhesive composite, indicating an observable connection between the bone/adhesive/screw. The surface bonding also affected cracks at the bone-adhesive interface, leading to more cracks through the trabeculae. The superior pullout resistance with the adhesive, with more distributed material and cracks compared to the brushite cement, indicates a potential benefit of this material to the initial implant stability.

## Declaration of Competing Interest

The following authors each declare partial ownership in a company

that owns all intellectual property related to the adhesive material studied in this paper, GPBio LTD: Michael Pujari-Palmer (M.P.-P.) and Philip Procter (P.P.).

## CRediT authorship contribution statement

**Dan Wu:** Investigation, Writing - original draft, Writing - review & editing. **Michael Pujari-Palmer:** Investigation, Writing - review & editing. **Alicja Bojan:** Investigation, Resources, Writing - review & editing. **Anders Palmquist:** Resources, Writing - review & editing. **Philip Procter:** Resources, Writing - review & editing. **Caroline Öhman-Mägi:** Investigation, Writing - review & editing. **Stephen J. Ferguson:** Resources, Writing - review & editing. **Per Isaksson:** Investigation, Resources, Conceptualization, Writing - review & editing, Supervision. **Cecilia Persson:** Investigation, Resources, Conceptualization, Writing - review & editing, Supervision, Funding acquisition.

## Acknowledgements

## Appendix A. Supplementary data

Supplementary data to this article can be found online at https://doi.org/10.1016/j.jmbbm.2020.103897.

## Funding

## References

Bai, B., Kummer, F.J., Spivak, J., 2001. Augmentation of anterior vertebral body screw fixation by an injectable, biodegradable calcium phosphate bone substitute. Spine 26, 2679–2683.

Barth, H.D., Zimmermann, E.A., Schaible, E., Tang, S.Y., Alliston, T., Ritchie, R.O., 2011. Characterization of the effects of X-ray irradiation on the hierarchical structure and mechanical properties of human cortical bone. Biomaterials 32, 8892–8904.

Brown, C.J., Sinclair, R.A., Day, A., Hess, B., Procter, P., 2013. An approximate model for cancellous bone screw fixation. Comput Method Biomec 16, 443–450.

Cornell, C.N., 2003. Internal fracture fixation in patients with osteoporosis. J. Am. Acad. Orthop. Surg. 11, 109–119.

Elder, B.D., Lo, S.-F.L., Holmes, C., Goodwin, C.R., Kosztowski, T.A., Lina, I.A., Locke, J. E., Witham, T.F., 2015. The biomechanics of pedicle screw augmentation with cement. Spine J. 15, 1432–1445.

Engstrand, J., Persson, C., Engqvist, H., 2014. The effect of composition on mechanical properties of brushite cements. J. Mech. Behav. Biomed. 29, 81–90.

Frankel, B.M., D'Agostino, S., Wang, C., 2007. A biomechanical cadaveric analysis of polymethylmethacrylate-augmented pedicle screw fixation. J. Neurosurg. Spine 7, 47–53.

Gibson, L.J., 1985. The mechanical behaviour of cancellous bone. J. Biomech. 18, 317–328.

Gibson, L.J., Ashby, M.F., 1997. Cellular Solids: Structure and Properties, 2 ed. Cambridge University Press, Cambridge.

Hoppe, S., Loosli, Y., Baumgartner, D., Heini, P., Benneker, L., 2014. Influence of screw augmentation in posterior dynamic and rigid stabilization systems in osteoporotic lumbar vertebrae: a biomechanical cadaveric study. Spine 39, E384–E389.

Joffre, T., Isaksson, P., Procter, P., Persson, C., 2017. Trabecular deformations during screw pull-out: a micro-CT study of lapine bone. Biomech. Model. Mechanobiol. 16, 1349–1359.

Katonis, P., Papadakis, S.A., Galanakos, S., Paskou, D., Bano, A., Sapkas, G., Hadjipavlou, A.G., 2011. Lateral mass screw complications: analysis of 1662 screws. Clinic. Spine Surg. 24, 415–420.

Kim, S.-J., Park, H.-S., Lee, D.-W., Lee, J.-W., 2018. Is calcium phosphate augmentation a viable option for osteoporotic hip fractures? Osteoporos. Int. 29, 2021–2028.

Larsson, S., Bauer, T.W., 2002. Use of injectable calcium phosphate cement for fracture fixation: a review. Clin. Orthop. Relat. Res. 395, 23–32.

Larsson, S., Stadelmann, V.A., Arnoldi, J., Behrens, M., Hess, B., Procter, P., Murphy, M., Pioletti, D.P., 2012. Injectable calcium phosphate cement for augmentation around cancellous bone screws. In vivo biomechanical studies. J. Biomech. 45, 1156–1160.

Lattig, F., 2009. Bone cement augmentation in the prevention of adjacent segment failure after multilevel adult deformity fusion. J. Spinal Disord. Tech. 22, 439–443.

Leung, K.S., Siu, W.S., Li, S.F., Qin, L., Cheung, W.H., Tam, K.F., Lui, P.P.Y., 2006. An in vitro optimized injectable calcium phosphate cement for augmenting screw fixation in osteopenic goats. J. Biomed. Mater. Res. B Appl. Biomater. 78B, 153–160.

Liu, D., Wu, Z.-x., Pan, X.-m., Fu, S.-c., Gao, M.-x., Shi, L., Lei, W., 2011. Biomechanical comparison of different techniques in primary spinal surgery in osteoporotic cadaveric lumbar vertebrae: expansive pedicle screw versus polymethylmethacrylate-augmented pedicle screw. Arch. Orthop. Trauma Surg. 131, 1227–1232.

Liu, X., Pujari-Palmer, M., Wenner, D., Procter, P., Insley, G., Engqvist, H., 2019. Adhesive cements that bond soft tissue ex vivo. Materials 12, 2473.

Lucksanasombool, P., Higgs, W.A., Ignat, M., Higgs, R.J., Swain, M.V., 2003. Comparison of failure characteristics of a range of cancellous bone-bone cement composites. J. Biomed. Mater. Res. 64, 93–104.

Maquer, G., Musy, S.N., Wandel, J., Gross, T., Zysset, P.K., 2015. Bone volume fraction and fabric anisotropy are better determinants of trabecular bone stiffness than other morphological variables. J. Bone Miner. Res. 30, 1000–1008.

McKoy, B.E., An, Y.H., 2000. An injectable cementing screw for fixation in osteoporotic bone. J. Biomed. Mater. Res. 53, 216–220.

Moore, D.C., Maitra, R.S., Farjo, L.A., Graziano, G.P., Goldstein, S.A., 1997. Restoration of pedicle screw fixation with an in situ setting calcium phosphate cement. Spine 22, 1696–1705.

Okuyama, K., Abe, E., Suzuki, T., Tamura, Y., Chiba, M., Sato, K., 2001. Influence of bone mineral density on pedicle screw fixation: a study of pedicle screw fixation augmenting posterior lumbar interbody fusion in elderly patients. Spine J. 1, 402–407.

Paré, P.E., Chappuis, J.L., Rampersaud, R., Agarwala, A.O., Perra, J.H., Erkan, S., Wu, C., 2011. Biomechanical evaluation of a novel fenestrated pedicle screw augmented with bone cement in osteoporotic spines. Spine 36, E1210–E1214.

Peña Fernández, M., Cipiccia, S., Dall'Ara, E., Bodey, A.J., Parwani, R., Pani, M., Blunn, G.W., Barber, A.H., Tozzi, G., 2018. Effect of SR-microCT radiation on the mechanical integrity of trabecular bone using in situ mechanical testing and digital volume correlation. J. Mech. Behav. Biomed. 88, 109–119.

Piper, A., Brown, C.J., 2016. A computational approximation to model variation in cancellous bone screw pull-out. J. Med. Dev. Trans. ASME 10, 021001-021001-021007.

Pishnamaz, M., Lange, H., Herren, C., Na, H.-S., Lichte, P., Hildebrand, F., Pape, H.-C., Kobbe, P., 2018. The quantity of bone cement influences the anchorage of augmented pedicle screws in the osteoporotic spine: a biomechanical human cadaveric study. Clin. BioMech. 52, 14–19.

Procter, P., Bennani, P., Brown, C.J., Arnoldi, J., Pioletti, D.P., Larsson, S., 2015. Variability of the pullout strength of cancellous bone screws with cement augmentation. Clin. BioMech. 30, 500–506.

Procter, P., Pujari-Palmer, M., Hulsart-Billström, G., Wenner, D., Insley, G., Larsson, S., Engqvist, H., 2019. A biomechanical test model for evaluating osseous and osteochondral tissue adhesives. BMC Biomed. Eng. 1, 11.

Pujari-Palmer, M., Guo, H., Wenner, D., Autefage, H., Spicer, C.D., Stevens, M.M., Omar, O., Thomsen, P., Edén, M., Insley, G., Procter, P., Engqvist, H., 2018a. A novel class of injectable bioceramics that glue tissues and biomaterials. Materials 11, 2492.

Pujari-Palmer, M., Robo, C., Persson, C., Procter, P., Engqvist, H., 2018b. Influence of cement compressive strength and porosity on augmentation performance in a model of orthopedic screw pull-out. J. Mech. Behav. Biomed. 77, 624–633.

Reitman, C.A., Nguyen, L., Fogel, G.R., 2004. Biomechanical evaluation of relationship of screw pullout strength, insertional torque, and bone mineral density in the cervical spine. J. Spinal Disord. Tech. 17, 306–311.

Renner, S.M., Lim, T.H., Kim, W.J., Katolik, L., An, H.S., Andersson, G.B., 2004. Augmentation of pedicle screw fixation strength using an injectable calcium phosphate cement as a function of injection timing and method. Spine 29, E212–E216.

Sarzier, J.S., Evans, A.J., Cahill, D.W., 2002. Increased pedicle screw pullout strength with vertebroplasty augmentation in osteoporotic spines. J. Neurosurg. Spine 96, 309–312.

Schliemann, B., Risse, N., Frank, A., Müller, M., Michel, P., Raschke, M.J., Katthagen, J. C., 2019. Screws with larger core diameter and lower thread pitch increase the stability of locked plating in osteoporotic proximal humeral fractures. Clin. BioMech. 63, 21–26.

Seebeck, J., Goldhahn, J., Stadele, H., Messmer, P., Morlock, M.M., Schneider, E., 2004. Effect of cortical thickness and cancellous bone density on the holding strength of internal fixator screws. J. Orthop. Res. 22, 1237–1242.

Seeherman, H.J., Bouxsein, M., Kim, H., Li, R., Li, X.J., Aiolova, M., Wozney, J.M., 2004. Recombinant human bone morphogenetic protein-2 delivered in an injectable calcium phosphate paste accelerates osteotomy-site healing in a nonhuman primate model. J. Bone Joint Surg. 86-a, 1961–1972. American Volume.

Shea, T.M., Laun, J., Gonzalez-Blohm, S.A., Doulgeris, J.J., Lee, W.E., Aghayev, K., Vrionis, F.D., 2014. Designs and techniques that improve the pullout strength of pedicle screws in osteoporotic vertebrae: current status. BioMed Res. Int. 15, 2014.

Singh, M., Nagrath, A.R., Maini, P.S., 1970. Changes in trabecular pattern of the upper end of the femur as an index of osteoporosis. J. Bone Jt. Surg. Am. Vol. 52, 457–467.

Stankewich, C.J., Swiontkowski, M.F., Tencer, A.F., Yetkinler, D.N., Poser, R.D., 1996. Augmentation of femoral neck fracture fixation with an injectable calcium-phosphate bone mineral cement. J. Orthop. Res. 14, 786–793.

Tassani, S., Öhman, C., Baleani, M., Baruffaldi, F., Viceconti, M., 2010. Anisotropy and inhomogeneity of the trabecular structure can describe the mechanical strength of osteoarthritic cancellous bone. J. Biomech. 43, 1160–1166.

Wang, W., Baran, G.R., Garg, H., Betz, R.R., Moumene, M., Cahill, P.J., 2009. The benefits of cement augmentation of pedicle screw fixation are increased in osteoporotic bone: a finite element analysis. Spine Deformity 2, 248–259.

Wirth, A.J., Goldhahn, J., Flaig, C., Arbenz, P., Müller, R., van Lenthe, G.H., 2011. Implant stability is affected by local bone microstructural quality. Bone 49, 473–478.

Yu, B.-S., Li, Z.-M., Zhou, Z.-Y., Zeng, L.-W., Wang, L.-B., Zheng, Z.-M., Lu, W.W., 2011. Biomechanical effects of insertion location and bone cement augmentation on the anchoring strength of iliac screw. Clin. BioMech. 26, 556–561.